Journal of Nuclear Materials 390–391 (2009) 1–9

Contents lists available at ScienceDirect

Journal of Nuclear Materials

journal homepage: www.elsevier.com/locate/jnucmat

Recent analysis of key plasma wall interactions issues for ITER

Joachim Roth [a,*], E. Tsitrone [b], A. Loarte [d], Th. Loarer [b], G. Counsell [h], R. Neu [a], V. Philipps [c], S. Brezinsek [c], M. Lehnen [c], P. Coad [e], Ch. Grisolia [b], K. Schmid [a], K. Krieger [a], A. Kallenbach [a], B. Lipschultz [j], R. Doerner [f], R. Causey [g], V. Alimov [i], W. Shu [i], O. Ogorodnikova [a], A. Kirschner [c], G. Federici [h], A. Kukushkin [d], EFDA PWI Task Force, ITER PWI Team, Fusion for Energy, ITPA SOL/DIV

[a] Max-Planck-Institut für Plasmaphysik, EURATOM-Association, 85748 Garching, Germany
[b] Association Euratom-CEA, CEA/DMS/DRFC CEA Cadarache, 13108 St. Paul-lez-Durance, France
[c] Institut für Plasmaphysik, Forschungszentrum Jülich GmbH, EURATOM-Association, 52425 Jülich, Germany
[d] ITER Organization, Fusion Science and Technology Department, Cadarache, 13108 St. Paul-lez-Durance, France
[e] EURATOM/UKAEA Fusion Association, Culham Science Centre, Abingdon, Oxon OX14 3DB, United Kingdom
[f] Fusion Energy Research Program, University of California–San Diego, Gillman Drive 9500, La Jolla, CA 92093-0417, USA
[g] Sandia National Lababoratory, P.O. Box 969, Livermore, CA 94550, USA
[h] Fusion for Energy, ITER Department, 08019 Barcelona, Spain
[i] Japan Atomic Energy Agency, Tritium Technology Group, Tokai, Ibaraki 319-1195, Japan
[j] Massachusetts Institute of Technology, Plasma Science and Fusion Center, 175 Albany St., Cambridge, MA, USA

A B S T R A C T

Plasma wall interaction (PWI) is important for the material choice in ITER and for the plasma scenarios compatible with material constraints. In this paper, different aspects of the PWI are assessed in their importance for the initial wall materials choice: CFC for the strike point tiles, W in the divertor and baffle and Be on the first wall. Further material options are addressed for comparison, such as W divertor/Be first wall and all-W or all-C. One main parameter in this evaluation is the particle flux to the main vessel wall. One detailed plasma scenario exists for a $Q = 10$ ITER discharge [G. Federici et al., J. Nucl. Mater. 290–293 (2001) 260] which was taken as the basis of further erosion and tritium retention evaluations. As the assessment of steady state wall fluxes from a scaling of present fusion devices indicates that global wall fluxes may be a factor of 4 ± 3 higher, this margin has been adopted as uncertainty of the scaling. With these wall and divertor fluxes, important PWI processes such as erosion and tritium accumulation have been evaluated: It was found that the steady state erosion is no problem for the lifetime of plasma-facing divertor components. Be wall erosion may pose a problem in case of a concentration of the wall fluxes to small wall areas. ELM erosion may drastically limit the PFC lifetime if ELMs are not mitigated to energies below 0.5 MJ. Dust generation is still a process which requires more attention. Conversion from gross or net erosion to dust and the assessment of dust on hot surfaces need to be investigated. For low-Z materials the build-up of the tritium inventory is dominated by co-deposition with eroded wall atoms. For W, where erosion and tritium co-deposition are small, the implantation, diffusion and bulk trapping constitute the dominant retention processes. First extrapolations with models based on laboratory data show small contributions to the inventory. For later ITER phases and the extrapolation to DEMO additional tritium trapping sites due to neutron-irradiation damage need to be taken into account. Finally, the expected values for erosion and tritium retention are compared to the ITER administrative limits for the lifetime, dust and tritium inventory.

1. Introduction

Since the last PSI conference in 2006, the ITER Joint Implementing Agreement has been signed by the seven partners of the project, allowing to launch the construction of the machine [2,3]. By end 2006, a design review process has been started, including discussion of urgent plasma wall interactions (PWI) issues, in particular those needing evaluation for the licensing authorities. The most critical PWI issues have been identified as:

- lifetime of plasma-facing components (PFCs);
- dust production from eroded PFCs;
- tritium (T) inventory in the vacuum vessel.

* Corresponding author.
E-mail address: roth@ipp.mpg.de (J. Roth).

0022-3115/$ - see front matter © 2009 Elsevier B.V. All rights reserved.
doi:10.1016/j.jnucmat.2009.01.037

This paper presents an assessment of these issues performed during the design review process through the European Plasma Wall Interaction Task Force (EU PWI TF) and, for the case of tritium retention in W, the US Burning Plasma Office (BPO).

In the evaluation of the above issues, which determine the choice of PFC materials (such as carbon fibre composite (CFC), tungsten (W), or beryllium (Be)) for reliable and safe operation of ITER, less emphasis was set on the detailed understanding of individual physical processes – previous reviews will be referenced throughout the paper – than on the consolidation of these individual processes in establishing robust predictions and associated uncertainty margins.

In Section 2 of this paper, ITER safety limits for PWI issues, such as T and dust inventories, are reviewed. In Section 3, input parameters used for the assessment, as well as material options considered, are described. Section 4 presents the assessment of erosion of PFCs, both from steady state and transient loads. Erosion rates derived in Section 4 are then used to evaluate dust generation in Section 5, and T inventory in Section 6. Different material options are addressed for comparison (CFC divertor/W baffles + dome/Be first wall, W divertor/Be first wall, full-W, full-C). Finally, consequences for the plasma scenarios and the PFC material choice are summarised in Section 7.

2. PWI related safety issues for ITER

Although not a concern in present day tokamaks, in vessel dust and tritium inventories have been recognised as a safety and operational issue for next step devices such as ITER [4,5]. Safety related issues concerning mobilisable in vessel dust (size between 100 nm and 100 μm) inventory include:

- contribution to the in vessel T inventory;
- potential radioactive (mainly W) and toxic (Be) source term in case of accidental release in the environment;
- potential hydrogen production from the reaction with steam after an accidental water leak;
- potential dust explosion following hydrogen production and an accidental air ingress.

The mobilisable radioactive in vessel T inventory must be kept as low as reasonably achievable, in order to minimize the impact on the environment in case of accidental release, in particular to avoid the evacuation of the neighbouring population.

Maximum levels for mobilisable dust and T inventories have therefore been defined during the safety analysis of the ITER project:

- One kilogram for the mobilisable T in vessel inventory, driven by the 'no evacuation' limit.
- One ton of mobilisable dust in the vessel during the D–D and D–T phase, driven by estimate of the radioactive source term. No limit is foreseen during the H phase, as no significant activation/T inventory is expected.
- 6 kg of C, 6 kg of W, 6 kg of Be dust on hot surfaces, driven by the H production risk. This corresponds to the maximum allowable H quantity (2.5 kg) for the vessel integrity to be guaranteed in case of explosion. A complete oxidation of Be at 400 °C and C at 600 °C is assumed for the calculation. If no C is present in the machine, the limits are relaxed to 11 kg for Be, or 230 kg for W.

Administrative limits have been derived from these safety limits taking into account the uncertainties of the available measurement methods:

Table 1
Safety and administrative limits for tritium and dust in vessel inventories taken into account in this study.

	Safety limits	Administrative limit
In vessel T inventory	1 kg	700 g
Global in vessel dust inventory	1 ton	670 kg
Dust on hot surfaces	6 kg of C, 6 kg of W, 6 kg of Be If no C present, 11 kg for Be, and 230 kg for W*	No assessment available

* ITER Organisation has recently (2009) reduced this limit to 77 kg W.

- Estimates of the in vessel dust inventory rely on measurements from the In Vessel Viewing System (IVVS), allowing to evaluate erosion from PFCs [6]. The accuracy of the IVVS on erosion measurements corresponds to ~300 kg of materials, currently being validated through an R&D plan [4]. Dust not easily recoverable during divertor replacement is estimated to 30 kg remaining almost constant with time. This leads to an administrative limit of ~670 kg assumed in this paper for the global mobilisable dust inventory allowed in the vacuum vessel (VV).
- The administrative limit for the dust on hot surfaces still has to be assessed. In this paper, we will therefore keep the safety limits given above.
- In the case of T inventory, uncertainties arise both from the estimates on the T burnt, and on the T accounting in the VV [7]. They are now evaluated to be ~180 g, reduced with respect to previous estimates [4]. Moreover, a T inventory of 120 g is allowed in the divertor cryopumps. Although the uncertainties will evolve with time, a constant administrative limit of ~700 g is assumed in this paper for the in vessel T inventory.

Table 1 summarises the safety and administrative limits considered in this paper.

3. Input parameters used

3.1. Input plasma parameters

Input plasma particle and energy fluxes, as well as surface temperatures, are taken for a reference 400 s Q = 10 ITER discharge as evaluated in [8] and used in [9]. The resultant fluxes are illustrated in Fig. 5 of Ref. [9].

In the divertor near the plasma strike point the typical ion and neutral fluxes reach values larger than $10^{24}\,m^{-2}\,s^{-1}$ (leading to a total fluence $>10^{26}\,m^{-2}$ for each ITER pulse) with divertor plasma densities $\sim10^{21}\,m^{-3}$ and plasma temperatures of ~3 eV. This corresponds to a D^+ impact energy of ~15 eV, due to acceleration in the plasma sheath potential. The expected surface temperature around the strike points is ~1300 K on the outer divertor, ~800 K on the inner divertor [1].

The estimates of *first wall* fluxes are more uncertain. The modelling results used here indicate that the D neutral flux is in the range of 10^{19}–$10^{21}\,m^{-2}\,s^{-1}$ with typical energies ~8–300 eV [8]. The ion fluxes are 3 orders of magnitude lower than at the divertor strike point and lie in the lower range of more recent estimates, taking into account long range transport across the SOL [10]. These estimates do not provide yet a consistent poloidal distribution, but indicate that wall fluxes may be a factor of 4 ± 3 higher than in Ref. [8], while the divertor fluxes remain similar. The evaluations in this paper are based on Ref. [8] for the divertor conditions, assuming a D/T ratio of 50/50%. For the wall particle fluxes, uncertainties are taken into account by using the results in [8] scaled to a total ion flux to the first wall between 1 and $7 \times 10^{23}\,s^{-1}$, in line with present empirical scalings of such parameter to ITER [10].

3.2. Material configuration

This review compares the four following options:

- *Option 1:* CFC divertor strike point tiles, W baffle and dome, and Be first wall.
- *Option 2:* W divertor/Be first wall.
- *Option 3*: Full-W device.
- *Option 4*: Full-C device.

Option 1 corresponds to the initial material selection for ITER PFCs, resulting largely from plasma wall interaction considerations. Option 2 has been proposed as the material choice for the activated phase of ITER, driven by minimization of the T inventory. The full-W option 3 is foreseen at a later stage in ITER when full power $Q = 10$ discharges are established and DEMO reactor conditions are investigated. This option requires the possibility of a change of the first wall material. The full-C option 4 is presently not included in the materials choices of ITER. As many of present day's devices are operated with all-C PFCs this option is included in this review for comparison.

In the subsequent work, the following material thicknesses have been considered [11]:

- Eighteen millimeter for CFC on the divertor strike points for option 1.
- Ten millimeter for the W baffle and dome for option 1, and for the W divertor and wall in options 2 and 3.
- Ten millimeter for the Be first wall in options 1 and 2.

In the scope of this review, the lifetime of a plasma-facing material is assumed to be reached when 2/3 of its initial thickness is eroded.

4. Lifetime of plasma-facing components

The first step in the chain of processes determining the PFCs lifetime, leading to dust generation and tritium retention by co-deposition, is the erosion of the wall material.

4.1. Erosion in steady state

Processes leading to erosion of plasma-facing materials have been recently summarised in [9]. The main features are:

- Erosion of Be and W by physical sputtering is largely covered and well described [12–14]. In the incident energy range below 1 keV, especially for light ions, threshold effects have to be considered [15,16].
- For carbon based materials, chemical interactions with hydrogen leads to enhanced erosion yields [17], reviewed in [18]. The chemical sputtering yield exhibits a maximum at elevated surface temperatures (around 10^{-1} at 600–800 K), a decrease at high incident fluxes (below 10^{-2} [19] above 10^{22} D/m^2 s), and a decrease towards a threshold energy (see Fig. 1). Despite this complex behaviour, the chemical erosion yield is adequately described by an empirical set of equations [19].
- C re-deposited layers experience an 'enhanced' chemical erosion with yields 10 times higher than for bulk graphite [20], as seen in laboratory experiments [21]. For deposited metals, such as Be, most evaluations use the same erosion yield as for bulk material. However, in recent laboratory deposition experiments with Be [22] an erosion yield enhanced by a factor of 2 was observed.

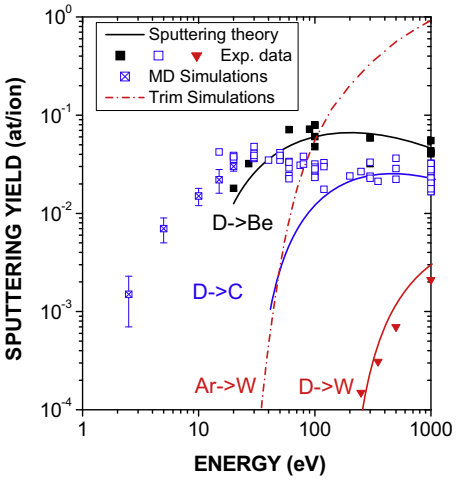

Fig. 1. Sputtering yields for C, Be and W bombarded with D ions [23]. For C, chemical erosion enhances the yield at low energies and yields are extrapolated to the threshold by MD calculations [87]. For W, impurity sputtering, such as Ar ions, dominates.

Table 2
Average and peak erosion rate for the ITER first wall, and associated PFC lifetime.

Wall material	Erosion rate (nm/s)	Erosion source (atoms/s)	Eroded material (g/shot)	Lifetime (shots)
Be (C) average	0.1	8×10^{21}	48	20 000
peak 50 m^2	4			5000
W average	0.01	2×10^{20}	26	200 000
peak 50 m^2	0.1			20 000

Taking the incident particle fluxes and energies from Section 3 (Ref. [8] with wall particle flux multiplied by 4 ± 3) and using known physical erosion yields [23], the wall net erosion rates can be calculated using the DIVIMP code [24] for sputtering of Be and W. Values for CFC are not given here, but are assumed to be very similar to Be in terms of erosion rates. Depending on details of the wall design, the erosion rate is given in Table 2 for a homogeneous distribution over the vessel wall according to Ref. [8] and alternatively for the assumption of a total wetted area of only 50 m^2.

The divertor erosion is evaluated using the ERO code, assuming the energy and particle fluxes given in [11], and including chemical erosion yields for carbon [19,20,25]. For W, erosion is calculated using DIVIMP and re-deposition fractions are estimated from experimental data from ASDEX Upgrade [26]. Values for gross and net erosion are given in Table 3 for CFC and W. The tables list erosion rates in nm/s, as relevant for the lifetime, and the eroded material in g/shot as relevant for dust generation.

Table 3
Gross and net erosion rate for the ITER divertor, and associated PFC lifetime.

Divertor mat.		Erosion rate (nm/s)	Erosion source (atoms/s)	Eroded material (g/shot)	Lifetime (shots)
CFC	Gross	100	4×10^{22}	330	200
	Net	1	4×10^{20}	3	20 000
W	Gross	2	4×10^{20}	48	10 000
	Net	0.3	6×10^{19}	7	60 000

4.2. Erosion due to transient loads [27]

In order to assess the effect of ELMs and disruptions on divertor materials, plasma guns [28–30] are used to provide realistic conditions [2] (i.e., adequate pulse duration and energy density), as transient heat loads expected in ITER are difficult to achieve in existing tokamaks. The most recent results from the QSPA facility, given in [32], are summarised below.

4.2.1. Erosion due to ELMs

Under ITER type I ELM-like heat loads, the CFC erosion, mainly due to erosion of the PAN fibres [30], starts at 0.5 MJ/m^2 while it is negligible below. The tungsten erosion is mainly due to melt layer movement and droplets ejection. Melting of the edges of W samples starts above 0.4 MJ/m^2, a value quite similar as for CFC. Moreover, even below the melting threshold for W, cracks appear under repetitive heat loads (100 repetitive pulses at 0.8 MJ/m^2). It is not clear at the moment whether cracks propagation will eventually saturate once stresses in the material are released.

To extrapolate results to ITER, where the main differences are the detailed target geometry and the strong magnetic field, modelling is used. PAN-fibre erosion starting at 0.5 MJ/m^2 was reproduced in good quantitative agreement with the modelling of PHEMOBRID-3D and PEGASUS codes including vapour shielding effects [31]. The tungsten erosion due to melt layer movement and droplets ejection was modelled and extrapolated to castellated surfaces using the MEMOS code [31].

In conclusion, for both CFC and W, ELMs in ITER should be limited to an energy density of 0.5 MJ/m^2 to avoid serious damage and limitations of PFCs lifetime, as has been recognised by the ITER team. In the remainder of the paper it is assumed that plasma scenarios with mitigated ELMs are developed (see Ref. [32]), such that damage limiting the PFC lifetime is avoided. Erosion due to additional particle fluxes to the PFC surfaces during ELMs mitigated to below 0.5 MJ/m^2 can be estimated to be much smaller than due to between-ELM fluxes [33] for the case of CFC and tritium retention by co-deposition due to ELMs can be neglected (Fig. 2). For the case of W the erosion depends on the concentration of impurities added for radiation cooling. Due to the low between-ELM erosion rate ELM erosion may contribute and is taken into account for dust production. The comparison in Fig. 2 is based on gross erosion neglecting re-deposition effects which are difficult to assess during ELMs.

4.2.2. Erosion due to disruptions

Thermal quench of a full-performance ITER plasma, with ≈350 MJ of thermal energy will result in significant transient heat loads causing vaporisation and melting of divertor material. Presently, assumptions for a worst-case ITER disruption thermal quench are [2,34,35]:

- energy loss 80–100% of the initial plasma thermal energy;
- a modest scrape-off layer (SOL) width expansion (~3);
- an inboard/outboard divertor energy ratio between 2:1 and 1:2;
- a toroidal energy peaking factor (peak/average ratio) up to 1.5.

This would lead to >10 GW m^{-2} at the divertor target for thermal quench times of the order of 1–3 ms, resulting in a vaporisation layer of the order of few μms for CFC [36–39]. In the case of tungsten a melt layer of several hundred μm could develop, part of which, if not all, could be lost. A key parameter in the life expectancy of the ITER target under disruptive thermal loads is the efficiency of the pre-disruption performance deterioration, which may set additional constraints on the choice of plasma scenarios.

However, disruptions in JET and ASDEX Upgrade seem less severe than derived from the previous assumptions [40,41], with a larger broadening of the SOL width (3–10) and a smaller fraction of the initial energy released during the thermal quench due to pre-disruption performance deterioration. These two key parameters determine the power loads and therefore the lifetime of PFCs due to disruptions. If this is confirmed, energy densities from standard ITER disruptions would be lower than presently assumed (typically 2–20 MJ/m^2, average 6 MJ/m^2), except for internal transport barrier (ITB) disruptions, where the fraction of energy released still seems to be close to 100%. Moreover, as analysed in JET [40], only a small fraction of the ITER disruptions will probably correspond to the reference worst case.

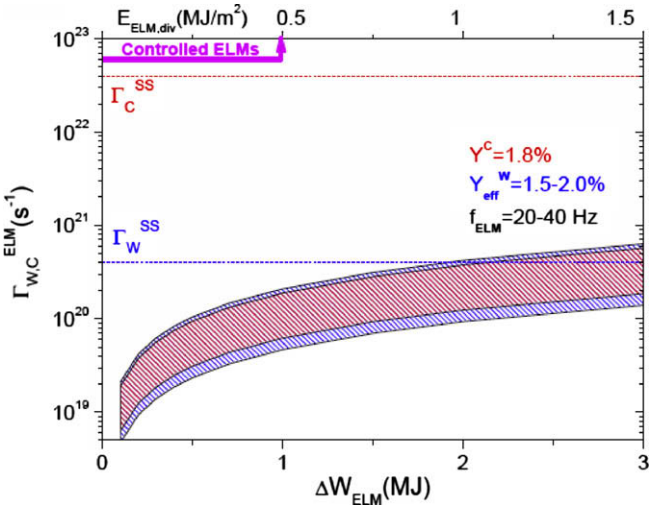

Fig. 2. Estimated erosion fluxes due to ELMs as function of ELM energy for CFC and W compared to the in-between-ELM erosion fluxes. ELM frequencies between 20 and 40 Hz were assumed [33]. ELM erosion is compared with gross steady state erosion.

ITER specifications indicate that divertor materials should support at least 300 disruptions [34]. Fig. 3 shows the erosion per disruption as a function of power density and thermal quench timescale for CFC and W as divertor materials [42]. The shaded region corresponds to the power density range of ITER disruptions as extrapolated from JET [40]. For CFC, erosion is reduced by a factor ~10 [43] due to vapour shielding, limiting evaporation and leading to a tolerable lifetime [42]. For W, where melt layers loss dominates, estimates from Fig. 3 show a lifetime lower than the

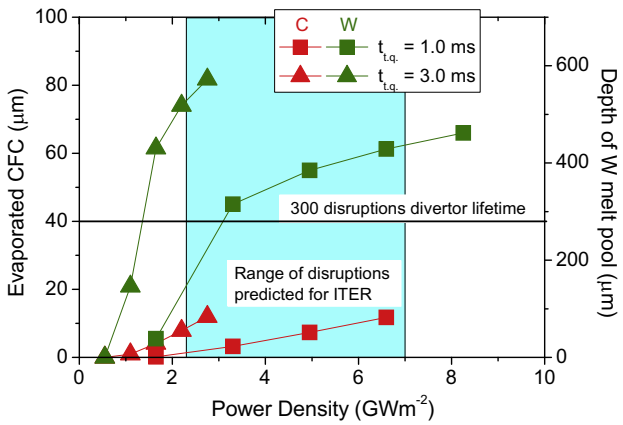

Fig. 3. Erosion of CFC and W per disruption as function of the transient heat load for transients of 1 and 3 ms as calculated using the RACLETTE code [42]. ITER disruption heat loads are expected in the shaded region [40]. For CFC, vapour shielding was taken into account reducing the sublimation rate by about one order of magnitude [43].

300 disruptions limit. Disruption mitigation techniques [44–46] have to be developed and the disruption frequency minimized. The present ITER assumption is 300 disruptions in 20000 discharges (1.5%), with a mass loss of PFC of ~5 kg per disruption [4]. These values are assumed throughout the remainder of the paper.

5. Dust generation

In tokamaks, dust can be produced during various operation phases:

- Layer deposition and disintegration in steady state.
- Disruptions.
- Arcing [47,48].
- Operations during maintenance phases.

In this study, we will only consider the first two points. Dust is formed either directly by erosion processes leading to ejection of particulates or droplets, or by delamination of re-deposited layers. In both cases the formation rate is primarily determined by the respective erosion rate, which also represents the upper limit of dust formation. Assessing the fraction of eroded material which will end up as mobilisable dust still requires a significant effort, both from the experimental (collection of dust in present day tokamaks) and modelling point of view. At present there are no sound empirical results available for the dust production conversion factor C_d (C_d = dust production/gross erosion). In present day machines, preliminary estimates yields a dust conversion factor of the order of 0.1 in JT60U and Tore Supra [49]. As a very conservative first estimate, one can take the gross erosion rate as an upper limit for dust production ($C_d = 1$). However, this is likely a large overestimate for dust production as one has to take into account:

- Local or prompt re-deposition, where the same atoms undergo multiple sputtering events before being deposited in remote areas. As an example, recent modelling of the ITER divertor with the ERO code for carbon transport yields a local re-deposition fraction as high as 99% [25] with a net erosion rate 100 times lower than the gross erosion rate.
- Only a fraction of the re-deposited layers will generate mobilisable dust. In general, thick re-deposited layers tend to flake under thermal stresses during plasma operation, but also when exposed to air during machine opening, making interpretation of post mortem analysis difficult.

However, we will still adopt here a conservative approach based on gross erosion estimates from previous sections.

5.1. Total dust generation

Fig. 4 presents the gross erosion calculated for different material options. Steady state erosion, as well as erosion due to disruption (assumption: 1 disruption every 66 shots leading to 5 kg of C/Be/W eroded, [4,50], see Section 4.2.2) are taken into account. The effect of disruption erosion is the same for all materials options, but is only shown for W (Fig. 4) where it dominates the erosion. ELMs are not included assuming ELM energy densities below the erosion threshold (see Section 4.2.1).

However, even taking the gross erosion rate as a conservative estimate of dust production, the total 'cold' dust limit of 1 ton for CFC/Be/W or full-C, as well as the 'hot' limit of 230 kg for W, or W/Be, are not reached before the maintenance period allowing for cleaning procedures to be applied. The main concern is then

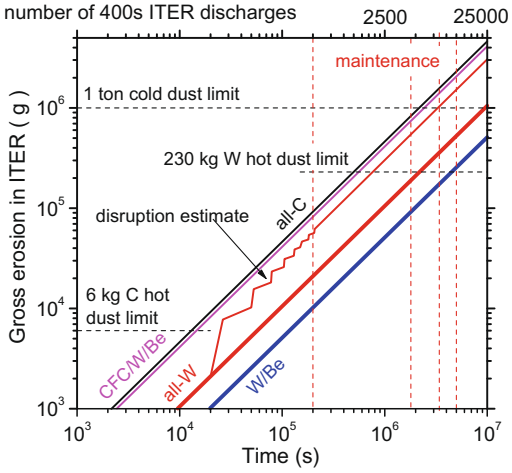

Fig. 4. Gross erosion for different materials options proposed for ITER calculated for steady state erosion compared to the different limits for dust for different materials. The additional tolerable erosion due to disruptions is indicated as example for the case of all-W PFCs.

the 'hot' dust limit of 6 kg for carbon, possibly reached in a few tens of discharges for the CFC/Be/W and full-C case.

5.2. Hot dust generation

Of particular concern is the hot area of the outer ITER divertor where the surface temperature lies in the range considered as problematic in the safety analysis. Experience in present day machines shows that the plasma wetted hot surfaces close to the plasma strike point are erosion dominated areas and remain free of deposited layers and dust [51,52]. Therefore, only the fraction of dust located in gaps of the divertor target needs to be considered.

The present ITER divertor design consists of macro-brush modules with a gap entrance fraction of about 2% of the total surface area. We will assume it to be the fraction of incoming impurities (including locally eroded target plate material as well as wall material transported from the main chamber) collected into the gaps. For a CFC divertor, taking gross erosion in Table 3, and assuming 2% entering the gaps and sticking there, leads to 6.6 g of carbon per discharge. Similarly, for the case of a tungsten target plate, this leads to 1 g/discharge of tungsten re-deposited in the gaps. In addition to these contributions, one has to take into account a flux of $2 \times 10^{19}/m^2$ s Be ions to the hot zone [53]. With a hot zone area of 8 m^2 this leads to 1.6×10^{20} Be/s $\approx$ 1 g/discharge deposited on the hot zone surface of which 0.02 g will be collected in gaps. The dust limit in the hot zone is therefore dominated by local deposition of eroded material.

It should be noted that only contributions from steady state erosion were considered. Erosion with direct dust formation by power transients is omitted here because power transients of that size must be avoided anyway to meet the lifetime requirements of PFCs.

5.3. Operational consequences

However, before becoming a safety concern, dust could be a potential operational issue. This has been seen in present day machines, when the thickness of deposited layers becomes significant and the film tends to flake under the thermal stresses imposed by plasma operation. For instance, after a campaign dedicated to wall deuterium loading in Tore Supra [54], using repetitive long pulses (5 h of plasma without intermediate conditioning), the main limitation came from bursts of impurities and

radiation ('UFOs') originating from the vessel walls and penetrating in the discharge, eventually leading to plasma detachment and disruptions. Analysis of these events has shown that they could be linked to the growth and flaking of deposited layers on plasma-facing components [55]. Although the issue could be attenuated in a divertor configuration with more efficient impurity screening, this new operational limit could be a serious concern for next step devices running repetitive discharges over long duration, leading to significant deposited layers thicknesses.

6. Tritium inventory

Tritium inventory accumulation in ITER has been the topic of a review published recently [9] using the same evaluation method as in the present paper. It will, therefore, be summarised here only shortly.

6.1. Implantation

Implantation and retention of low-energy hydrogen ions into pure materials, such as carbon [56,57], tungsten [58] and beryllium [59,60], have been investigated in detail and were summarised in [61]. Recently, the specific materials modifications proposed for application in fusion devices were also considered (e.g. CFC [66], vacuum plasma-sprayed (VPS) W [62]).

In Be and pyrolytic or fine grain graphites with low porosity, hydrogen does not diffuse and after reaching a local concentration in the implantation range of about 30 at.% further hydrogen is reemitted [60,63,64]. However, the behaviour is different in more porous materials [65], like in the CFC considered for ITER [66], where the retained amount increases close to a square root of the ion fluence due to diffusion deep into the bulk. As erosion and co-deposition for low-*Z* materials increases linearly with fluence and will dominate retention at long discharge durations, implantation is only relevant for W.

In W, deuterium is highly mobile and is only retained in radiation damage or defects of the crystal lattice [67,68]. After saturating available traps in the ion induced damage profile, inward diffusion and subsequent trapping at bulk lattice defects increases the trapped inventory. As the build-up of the inventory is diffusion limited, it increases with a quasi square-root dependence on the fluence. Fig. 5 shows modelling of the tritium inventory in W under ITER conditions [69,70] and predicts that it stays in tolerable limits for polycrystalline W in ITER neglecting n-irradiation damage. US [69] and EU [70] evaluations show very good agreement for unirradiated W.

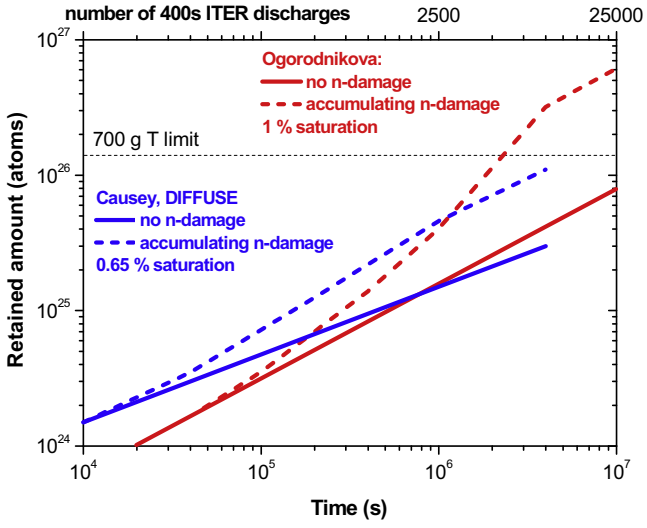

Fig. 5. Tritium inventory in W due to implantation, diffusion and trapping in the bulk as extrapolated from experimental data using different diffusion codes [68,73]. In addition to trapping in intrinsic and ion induced trapping sites also retention due to trapping in n-irradiation damage sites is estimated, assuming saturation trap concentrations of 1% [69] and 0.65% [70].

6.2. Influence of radiation damage due to n-irradiation

Already in ITER, but especially in DEMO the fuel retention properties of W plasma-facing materials will be enhanced due to radiation damage after high fluence n-irradiation, which provides additional trapping sites for hydrogen [71]. The irradiation damage at the end of the ITER lifetime has been estimated to 0.6 dpa in the divertor and 1dpa at the first wall [72], but the microstructure and its relation to hydrogen trapping is largely unknown. Simulations using the DIFFUSE code [73] build-up of n-induced trapping sites to a saturation value of 0.6% deduced very similar retention values as simulations in Ref. [70] assuming saturation at 1% (Fig. 5). In these calculations no ion induced trap generation has been taken into account due to the very shallow implantation depths leading to a retention increase with the square root of fluence. Consequently, a value of 700 g retained tritium will be reached after about 5000–10 000 discharges.

The saturation concentration of n-produced trap of 1% in W is an extreme upper limit and probably 0.1% is a more realistic value for ITER. Taking into account a saturation of damage sites at 0.01% after 0.6 dpa as reported for Mo [74], the additional trapping sites due to neutron damage might not be limiting throughout the lifetime of ITER. In addition, the density of n-induced vacancies will decrease with temperature by increasing the spontaneous annihilation and vacancy clustering. As such effects are not taken into account the present estimations give upper limits of T retention and need to be refined.

In spite of the coarse inclusion of the n-damage effect in the present modelling, both assessments show remarkable agreement. In both cases the unirradiated W retention is very similar, being dominated by the divertor areas at moderate fluxes and temperatures. Clearly, the additional effect due to n-damage requires more experimental validation and more detailed code simulation before a final conclusion can be drawn.

6.3. Co-deposition

Co-deposition is the incorporation of hydrogen in deposited layers where impurity atoms or molecules are deposited together with a flux of energetic or thermal hydrogen atoms. A collection of data on the deuterium concentration in C, Be and W deposits is shown in Fig. 6 [75].

For carbon deposited layers, the hydrogen concentration depends critically on the energy of the incident hydrogen flux. Energetic ions lead to the deposition of hard films with hydrogen concentrations H/C of about 0.4, while low energy or thermal hydrogen leads to the formation of soft films, with H/C concentrations exceeding 1 [76,77].

Similarly, recent analysis [78] shows structural changes in deposited Be layers for different energies of incident deuterium atoms and deposition rates, leading to low hydrogen content for low energies and high Be concentrations in the incident flux. In a recent analysis the D/Be ratio in deposited layers could be described by an empirical fit to data for different temperatures, ion energies and film deposition rates [79]. The role of oxygen in Be-rich co-deposits, which was originally thought to have a major impact [80], does not appear to play such a large role [81] compared to the temperature of the layer and the energy of the incident particles.

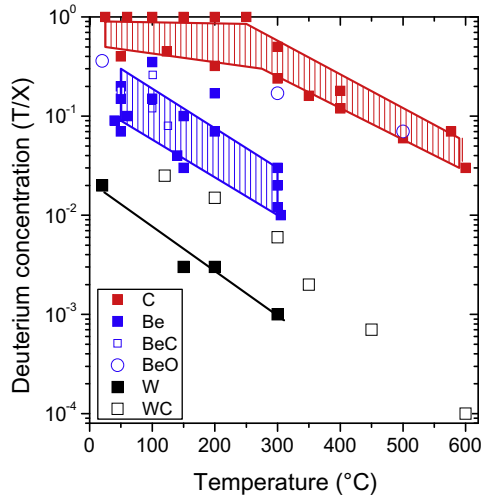

Fig. 6. Retained deuterium concentration in C, Be and W deposits under co-deposition conditions [75].

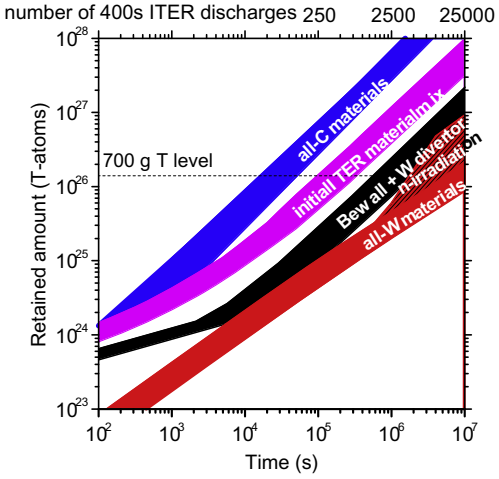

Fig. 7. Tritium inventory in ITER for the all-C (blue line) and all-W options (red line) compared to the initial material choice CFC/W/Be (magenta). In addition, retention values for the option of a full-W divertor and Be first wall are included (black line). The assessment was performed assuming different particle fluxes to different divertor and wall areas: divertor: 3 m^2, 2×10^{24} (D + T)/m^2 s, 775 K; 47 m^2, 2×10^{23} (D + T)/m^2 s, 500 K; baffle and wall: 750 m^2, $1–5 \times 10^{20}$ (D + T)/m^2 s, 380–440 K. The width of the bands indicates error margins essentially given by uncertainties in the incident wall fluxes. For W also an estimated contribution due to n-damage is introduced.

For deuterium co-deposition in W few data exist and the values are often close or below the detection limit of the measurements [80,75]. These low values combined with the very low erosion yields of W lead to the conclusion that co-deposition with W or WC will not be a critical process for ITER.

As is seen from above, predicting T retention in ITER is subject to large uncertainties, as local deposition conditions are difficult to assess: power and particle flux on the complex 3D geometry of PFCs, including gaps, composition of the incident flux in terms of fuel particles and impurities, local surface temperature, depending on the poorly characterised thermal properties of the layers.

The addition of the different tritium retention processes in Fig. 7 shows that the tritium inventory for the initial material choice CFC/W/Be will build-up mainly due to co-deposition with carbon and will reach the tritium limit within 100–300 full 400 s Q = 10 discharges.

An all-metal W/Be machine will result in a strongly reduced T build up compared to the initial material choice. Close to 3000 discharges are necessary to reach the T safety limit, now being dominated by the co-deposition with Be, mainly in the inner divertor.

For the all-C device, T co-deposition has been calculated using the ERO code [20] assuming an additional influx of 1% C ions into the divertor. The assumed T/C ratios in deposited layers were 0.2 in remote areas and 0.025 on the divertor plates. The resulting inventory agrees well with extrapolations from JET by scaling with the ion fluence to the divertor [82]. The global C influx, responsible for co-deposition, was calculated to 6×10^{21} C/s [20]. Clearly, in the all-C option, the T limit will be reached in a few tens of discharges and require frequent cleaning intervention.

The all-W extrapolation takes into account three different areas with differing ion flux and temperature in the divertor, baffle and first wall. The temperature of the wall is assumed to be around 400 K, while it is taken at 775 K in the divertor strike point area. The use of W in the divertor requires the extrapolation of experimental data over more than 2 orders of magnitude by computer modelling; numerical results are given in Fig. 7. The results show that the divertor strike point areas as well as the vessel wall areas contribute little to the inventory, because of the high temperatures or low ion fluxes, respectively. The main inventory will be build up in the divertor areas with intermediate flux (2×10^{23} (D + T)/m^2 s) and intermediate temperature (around 500 K). As expected, the lowest T retention is obtained for an all-W machine, where the inventory stays below the limit for >25 000 discharges. Additional traps for hydrogen in the W bulk due to n-irradiation provide a large uncertainty of the estimates and are indicated by the hatched area at long exposure times.

7. Consequences for plasma scenarios and material choice

From the estimates given above, the performance of different wall materials as well as limits on plasma scenarios can be discussed:

- Transient wall loading by ELMs and disruptions, which are usual in present fusion devices, must be strongly limited in ITER. Experimental studies of ELM-like power loads in linear plasma devices [30] have shown that both potential divertor materials, CFC and W, will erode strongly when the ELM energy density exceeds 0.5 MJ/m^2. Plasma scenarios with pellet pacemaking [83] or using edge ergodisation coils [84] have to be developed to meet this requirement. Even at this low load the high ELM frequency may cause embrittlement and cracking of W components and need to be studied in more detail. Similarly, disruptions need to be mitigated and strongly limited. The evaluations in this paper have been made assuming the ITER limitation of less than 3 disruptions for 200 discharges.

For steady state plasma conditions, Fig. 8 shows the estimated number of discharges for different material combinations until PFC lifetime, dust or tritium inventory limits are reached. The uncertainty margins for erosion and tritium retention arise from the large uncertainties in the estimates of wall fluxes. For dust generation the low margin is given by taking the gross erosion at the walls and divertor, the high margin considering reduced erosion due to re-deposition. In both cases, the hot dust limits were assumed:

- In terms of the lifetime of PFCs, steady state erosion is high for low-*Z* materials. For carbon in the divertor, re-deposition of eroded material reduces the net erosion resulting in component lifetime of about 10 000 discharges, i.e., longer than the foreseen exchange periods of the divertor cassettes [85]. Be as wall

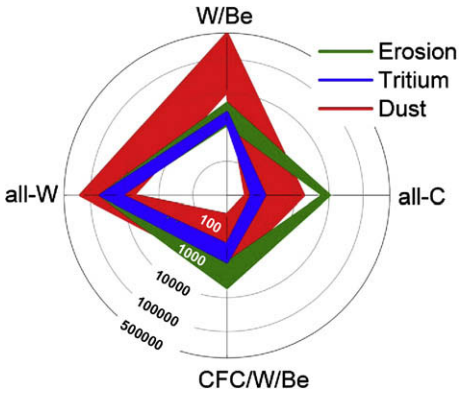

Fig. 8. Number of discharges required for reaching the safety limits due to erosion, dust generation and tritium inventory for the four material options for ITER. The origin of the error margins for each process is given in the text.

material also reaches similar numbers of discharges for a uniform loading of the vessel wall. However, if a non-homogeneous loading is assumed ($\frac{1}{2}$ of the wall flux on only 50 m^2), the lifetime may be reduced to 5000 discharges (see Table 2). As the exchange of wall material is by far more difficult in the present ITER design and only foreseen once in the ITER lifetime, this limit is very restricting. Improved wall design for more homogeneous loading and/or for easier replacement seems necessary. W in wall and divertor application has projected lifetimes well above 20000 discharges.

- As far as dust is concerned, the total mobilisable dust limit (1 ton in the vacuum vessel) appears not to be the limitation. However, the hot dust limit, being 6 kg for C, or 11 kg for Be (if no carbon is present), is more restrictive. If all eroded material is assumed to be deposited on hot, plasma heated surfaces – an assumption made to get an upper limit for the hot dust generation – short lifetimes of less than 100 discharges result. However, a closer investigation of hot dust generation is expected to strongly relax this limitation: On intensely plasma wetted areas, dust will not accumulate on the surface and will survive only in gaps. A rough estimate of material deposition in gaps increases this limit for carbon to several 1000 discharges and dust would be removed with the exchange of divertor cassettes. For the case of W/Be combination, dust generated due to Be wall erosion will reach the hot dust limit after 10000–500000 discharges. Dust generation estimates show the largest uncertainties. Dust generation mechanisms, conversion of deposited layers to dust, dust transport and mobilisation need to be studied in greater detail. However, dust could be an operational problem before becoming a safety limitation.
- The third safety limitation for ITER is the accumulation of mobilisable tritium in the vessel. In this case, the retention process dominating for low-Z materials with high erosion yield is co-deposition with eroded material, while for W implantation and bulk retention dominates. The most restricting tritium limit is evaluated for the material options involving carbon in the divertor with discharge numbers of 100–1000, requiring tritium removal methods in-between cassette exchanges [9]. The exchange of CFC divertor components to W leaves co-deposition of tritium with Be as the dominant retention mechanism. The limit is expected to be reached after 1500–3000 discharges and it is not clear, presently, whether the foreseen exchange of divertor cassettes will solve the problem. Closer investigations have to be made to determine the dominant location of Be/T co-deposition taking into account that local heating to 350 °C can recover up to 80% of the retained tritium. Implantation into W leads to tritium bulk retention reaching the limit within 10000–50000 discharges. During the last phase of ITER, n-irradiation of W will reduce this limit, but more experimental and modelling results are needed to better quantify this process [86].

From the standpoint of plasma wall interaction issues alone, and providing plasma scenarios with strongly reduced ELMs, no significant fast ions production, and mitigated disruptions can be achieved, an all-W device would solve best the lifetime, dust generation and tritium issues. Tritium, dust and erosion appear to be also tolerable for the W/Be option. However, the compatibility of the plasma scenarios required to reach the performance foreseen for ITER with W walls remains to be demonstrated.

References

[1] G. Federici et al., J. Nucl. Mater. 290–293 (2001) 260.
[2] ITER Physics Basis Editors et al., Nucl. Fus. 39 (1999) 2137.
[3] K. Ikeda et al., Nucl. Fus. 47 (2007).
[4] Sergio Ciattaglia, Rev.1, 01 April 2008.;
S. Ciattaglia, P. Andrew, A. Loarte, A. Martin, C.S. Pitcher, R. Pitts, S. Rosanvallon, M. Shimada, W. Shu, C.H. Skinner, A. Tesini, SOFT 2008, FED MsNr. FUSENGDES-D-08-00361, submitted for publication.
[5] S. Rosanvallon, C. Grisolia, P. Andrew, et al., J. Nucl. Mater., these Proceedings, doi:10.1016/j.jnucmat.2009.01.048.
[6] C. Neri et al., Fus. Eng. Des. 82 (2007) 2021.
[7] I.R. Cristescu, Forschungszentrum Karlsruhe Report, May 2007.
[8] A.S. Kukushkin, H.D. Pacher, V. Kotov, et al., Nucl. Fus. 45 (2005) 608.
[9] Joachim Roth, Emmanuelle Tsitrone, Thierry Loarer, Volker Philipps, Sebastijan Brezinsek, Alberto Loarte, Glenn F. Counsell, Russell P. Doerner, Klaus Schmid, Olga V. Ogorodnikova, Rion A. Causey, Plasma Phys. Control Fus. 50 (October) (2008) 103001.
[10] A. Kallenbach, A. Loarte, B. Lipschultz, Presented at the ITPA SOL/DIV in Avila, January 2008, private communication, 2007.
[11] ITER private communication, May 2008.
[12] P. Sigmund, Phys. Rev. 184 (1969) 383.
[13] R. Behrisch, W. Eckstein (Eds.), Sputtering by Particle Bombardment, Springer Verlag, Berlin, 2007.
[14] W. Eckstein, Springer Series in Materials Science, 1st Ed., Springer Verlag, Berlin, Heidelberg, 1991.
[15] J. Bohdansky, J. Roth, H.L. Bay, J. Appl. Phys. 51 (1980) 2861.
[16] J. Roth, J. Bohdansky, A.P. Martinelli, Radiat. Eff. 48 (1980) 213.
[17] J. Roth, J. Bohdansky, W. Poschenrieder, M.K. Sinha, J. Nucl. Mater. 63 (1976) 222.
[18] W. Jacob, J. Roth, in: R. Behrisch, W. Eckstein (Eds.), Sputtering by Particle Bombardment, Springer Verlag, Berlin, 2007.
[19] J. Roth, R. Preuss, W. Bohmeyer, S. Brezinsek, A. Cambe, E. Casarotto, R. Doerner, E. Gauthier, G. Federici, S. Higashijima, J. Hogan, A. Kallenbach, A. Kirschner, H. Kubo, J.M. Layet, T. Nakano, V. Philipps, A. Pospieszczyk, R. Pugno, R. Ruggiéri, B. Schweer, G. Sergienko, M. Stamp, Nucl. Fus. 44 (2004) L21.
[20] A. Kirschner et al., J. Nucl. Mater. 328 (2004) 62.
[21] E. Vietzke, A.A. Haasz, in: W.O. Hofer, J. Roth (Eds.), Physical Processes of the Interaction of Fusion Plasmas with Solids, Academic, San Diego, 1996.
[22] R. Doerner, M. Baldwin, private communication, 2007.
[23] W. Eckstein, C. Garcia-Rosales, J. Roth, W. Ottenberger, Report IPP 9/82, 1993.
[24] P.C. Stangeby, J.D. Elder, J. Nucl. Mater. 196–198 (1992) 258.
[25] A. Kirschner et al., J. Nucl. Mater. 390–391 (2009) 152.
[26] K. Krieger, H. Maier, R. Neu, ASDEX Upgrade Team, J. Nucl. Mater. 266–269 (1999) 207.
[27] A. Zhitlukhin, N. Klimov, I. Landman, J. Linke, A. Loarte, M. Merola, V. Podkovyrov, G. Federici, B. Bazylev, S. Pestchanyi, V. Safronov, T. Hirai, V. Maynashev, V. Levashov, A. Muzichenko, J. Nucl. Mater. 363–365 (2007) 301.
[28] V. Belan et al., J. Nucl. Mater. 233–237 (1996) 763.
[29] V. Belan et al., in: Proceedings of the 20th SOFT, Marseille, vol. 1, 7–11 September 1998, p. 101.
[30] N. Klimov, V. Podkovyrov, A. Zhitlukhin, D. Kovalenko, B. Bazylev, G. Janeschitz, I. Landman, S. Pestchanyi, G. Federici, A. Loarte, M. Merola, J. Linke, T. Hirai, J. Compan, J. Nucl. Mater. 390–391 (2009) 721.
[31] B.N. Bazylev, G. Janeschitz, I.S. Landman, A. Loarte, S.E. Pestchanyi, J. Nucl. Mater. 363–365 (2007) 1011.
[32] W. Fundamenski et al., J. Nucl. Mater. 390–391 (2009) 10.
[33] A. Loarte, private comminication, 2008.
[34] G. Federici et al., J. Nucl. Mater. 313–316 (2003) 11.
[35] J. Wesley, N. Fujisawa, S. Putvinski, M.N. Rosenbluth, in: Proceedings of the 17th Symposium on Fusion Engineering 1997, San Diego, 1997, vol. 1, IEEE, Piscataway, NJ, 1998, p. 483.
[36] H. Wuerz, S. Pestchanyi, B. Bazylev, F. Kappler, in: Proceedings of the 20th Symposium on Fusion and Technology, Marseille, France, vol. 1, 1998, p. 271.
[37] H. Wuerz et al., Fus. Eng. Des. 56&57 (2001) 349.
[38] H. Wuerz et al., Report Forschungszentrum Karlsruhe, FZKA 6582, 2001.
[39] A. Hassanein, I. Konkashbaev, J. Nucl. Mater. 273 (1999) 326.

[40] V. Riccardo, A. Loarte, the JET EFDA Conrtibutors, Nucl. Fus. 45 (2005) 427.
[41] P. Andrew et al., J. Nucl. Mater. 313–316 (2003) 135. Proceedings of the 30th EPS Conference 2003, St. Petersburg, Russia, 2003, p. 1.
[42] G. Federici, G. Strohmayer, 2007, unpublished.
[43] S. Pestchany et al., J. Nucl. Mater., these Proceedings, 2009.
[44] G. Pautasso et al., J. Nucl. Mater. 290–293 (2001) 1185.
[45] D. Whyte et al., J. Nucl. Mater. 313–316 (2003).
[46] G.F. Counsell et al., J. Nucl. Mater. 290–293 (2001) 255.
[47] S.A. Cohen, H.F. Dylla, S.M. Rossnagel, S.T. Picraux, J.A. Borders, C.W. Magee, J. Nucl. Mater. 76&77 (1978) 459.
[48] P. Staib, H. Kukral, E. Glock, G. Staudenmaier, J. Nucl. Mater. 111&112 (1982) 173.
[49] C. Grisolia, P. Sharpe, A. Loarte, S. Rosanvallon, J. Roth, B. Lipschultz, V. Rohde, D. Whyte, J. Nucl. Mater. 390–391 (2009) 53.
[50] S. Cattaglia, SOFT 2008, submitted for publication.
[51] M. Mayer, J. Likonen, J.P. Coad, et al., J. Nucl. Mater. 363–365 (2007) 102.
[52] M. Mayer, V. Rohde, G. Ramos, et al., Phys. Scr. T111 (2004) 49.
[53] K. Schmid, Presentation at ITPA SOL/DIV meetings Tarragona, 2005, Garching, 2007, private communication.
[54] B. Pégourié et al., J. Nucl. Mater. 390–391 (2009) 550.
[55] A. Ekedahl et al., J. Nucl. Mater. 390–391 (2009) 806.
[56] W.R. Wampler, C.W. Magee, J. Nucl. Mater. 103&104 (1981) 509.
[57] B.M.U. Scherzer, M. Wielunski, W. Möller, A. Turos, J. Roth, Nucl. Instrum. and Meth. B 33 (1988) 714.
[58] R. Causey, K. Wilson, T. Venhaus, W.R. Wampler, J. Nucl. Mater. 266–269 (1999) 467.
[59] W. Möller, B.M.U. Scherzer, J. Bohdansky, IPP-JET Report No. 26, 1985.
[60] R.A. Anderl, R.A. Causey, J.W. Davis, et al., J. Nucl. Mater. 273 (1999) 1.
[61] V.Kh. Alimov, J. Roth, Phys. Scr. T128 (2007) 6.
[62] A. Golubeva, V.A. Kurnaev, M. Mayer, J. Roth, in: G.R. Myneni, B. Hjörvarsson (Eds.), Hydrogen in Matter, AIP Conference Proceedings, vol. 837, American Institute of Physics, Melville, NY, 2006, p. 12.
[63] M. Reinelt, Ch. Linsmeier, private communication, 2007.
[64] B.L. Doyle, W.R. Wampler, D.K. Brice, S.T. Picraux, J. Nucl. Mater. 93&94 (1980) 551.
[65] A.A. Haasz, J. Davis, J. Nucl. Mater. 209 (1994) 1140.
[66] J. Roth, V.Kh. Alimov, A.V. Golubeva, R.P. Doerner, J. Hanna, E. Tsitrone, Ch. Brosset, V. Rohde, A. Herrmann, M. Mayer, J. Nucl. Mater. 363–365 (2007).
[67] R.A. Causey, T.J. Venhaus, Phys. Scr. T94 (2001) 9.
[68] O. Ogorodnikova, J. Roth, M. Mayer, J. Nucl. Mater. 313–316 (2003) 469.
[69] A.A. Haasz et al., US BPO Report, 2007.
[70] O. Ogorodnikova, ITPA SOL/DIV Garching, 2007.
[71] N. Baluc, Final Report on EFDA Task TW1-TTMA-002 Del. 5: Assessment report on W, 2001.
[72] Materials Assessment Report G 74 MA 10 01-07-11 W, Ch. 2.2 Tungsten, ITER, 2001.
[73] M.I. Baskes, Sandia Nat. Lab. Livermore, Report SAND80-8201, 1980.
[74] M. Eldrup, M. Li, L. Snead, S. Zinkle, Presented at the ICFRM 13, Nice J. Nucl. Mater., submitted for publication.
[75] R.P. Doerner, M.J. Baldwin, G. De Temmerman, J. Hanna, D. Nishijima, J. Roth, K. Schmid, G.R. Tynan, K. Umstadter, IAEA Genova, submitted for publication.
[76] T. Schwarz-Selinger, A. von Keudell, W. Jacob, J. Appl. Phys. 86 (1999) 3988.
[77] W. Jacob, Thin Solid Films 326 (1998) 1.
[78] R. Doerner, ITPA Garching, 2007, unpublished.
[79] G. DeTemmerman et al., J. Nucl. Mater. 390–391 (2009) 564.
[80] M. Mayer et al., J. Nucl. Mater. 240 (1997) 164.
[81] M. Baldwin et al., J. Nucl. Mater. 337–339 (2005) 590.
[82] Th. Loarer, J. Nucl. Mater. 390–391 (2009) 20.
[83] A. Kallenbach, P.T. Lang, R. Dux, et al., J. Nucl. Mater. 337–339 (2005) 732.
[84] M. Becoulet, G. Huysmans, P. Thomas, et al., J. Nucl. Mater. 337–339 (2005) 677.
[85] ITER N 94 PL 4 R0.2, ITER documentation, 2004.
[86] J. Roth, J. Davis, R. Doerner, A. Haasz, A. Kallenbach, A. Kirschner, R. Kolasinski, B. Lipschultz, A. Loarte, O. Ogorodnikova, V. Philipps, K. Schmid, W. Wampler, G. Wright, D. Whyte, A new look at the specification of ITER plasma wall interaction and tritium retention, Contribution to the 22nd IAEA Fusion Energy Conference, Geneva, 2008.
[87] A.V. Krasheninnikov, K. Nordlund, E. Salonen, J. Keinonen, C.H. Wu, Comput. Mater. Sci. 25 (2002) 427.